FERMILAB-PUB-15-296-PPD
ACCEPTED

Direct tests of micro channel plates as the active element of a new shower maximum detector

A. Ronzhin[a]*, S. Los[a], E. Ramberg[a], A. Apresyan[b], S. Xie[b], M. Spiropulu[b], H. Kim[c]

[a]*Fermilab, Batavia, Il 60510, USA,*

[b]*California Institute of Technology, Pasadena, CA, USA*

[c]*University of Chicago, Chicago, Il 60637, USA*

Abstract

We continue the study of micro channel plates (MCP) as the active element of a shower maximum (SM) detector. We present below test beam results obtained with MCPs detecting directly secondary particles of an electromagnetic shower. The MCP efficiency to shower particles is close to 100%. The time resolution obtained for this new type of the SM detector is at the level of 40 ps.

Keywords

Time Resolution or TR

---

* Corresponding author. Tel.: 1 630 840 8630

E-mail address: ronzhin@fnal.gov (A. Ronzhin)

Operated by Fermi Research Alliance, LLC under Contract No. De-AC02-07CH11359 with the United States Department of Energy.

1. Introduction

We first proposed in 1990 to use electron multipliers, like micro channel plates (MCPs), venetian blinds, or compact meshes dynode systems used in photomultipliers as an active element in SM detectors or in sandwich type calorimeters [1]. This approach allows one to develop a new type of a detector that is radiation resistant and fast. Such a detector could be implemented in future high energy physics experiments as a calorimetric device, enabling a simultaneous measurement of the time and energy of showering particles, such as electrons and photons.

We have shown [1] that MCPs produce fast and high amplitude signals, when irradiated by secondary particles from an electromagnetic shower, but the main limitation to introduce this technique into high energy physics experiments was the high cost of MCPs. With the recent progress of the Large Area Picosecond Photo Detector collaboration [2], the costs may decrease sufficiently.

In our previous articles [3, 4,] we presented general characteristics of a shower maximum detector (SM), namely, energy response, energy and position resolution, e^-/π^- rejection power, π^0/γ separation, which have been measured and calculated for different SM locations (depths) inside an electromagnetic calorimeter. The development of the shower and particles produced in absorbers is well described in [5, 6]. In our current work we concentrate on the study of the SM timing properties.

We obtained data [7] indicating that the shower particles were registered through the Cherenkov radiation in the input window of the Photonis XP85011 as well as through direct interaction with its MCP. As a follow up of the previous study, we obtained a Photonis XP85012 [8] MCP-PMT, which allows us to distinguish between these two types of detector interactions explicitly. We modified the standard Photonis XP85012 [8] MCP-PMT high voltage (HV) divider for this purpose. The customized HV divider allows us to change the potential between the photocathode (PC) and the MCP facing the PC. We made measurements clearly showing different behavior in the output signal depending on the potential applied between the PC and the MCP.

We made another HV divider allowing us to effectively eliminate photoemission of photoelectrons from the PC. A switch was introduced into the divider with the purpose of having two operational modes. One of the switch positions corresponds to normal MCP-PMT operation, which we refer in the following as the "PC ON" mode. The second mode allows us to operate the detector in MCP-only mode, where photoelectrons produced in the PC are prevented from reaching the MCP and producing a signal. We refer to this operational mode as "PC OFF". In the measurements described below we use both of these options. The PC ON mode was used mostly for calibration purposes. The goal of measurements performed at the Fermilab test beam was to characterize the efficiency of the MCP shower detection, and its timing properties. The results are presented below.

The paper is organized as follows. Section 1 is an introduction. In Section 2 we describe the

general properties of the Photonis XP85012. In Section 3 we present the customized Photonis XP85012 HV dividers including the schematics of the customized HV divider for both PC ON and PC OFF operational modes. In Section 4 we present the procedure and the result of our study of the influence of the potential applied between the PC and its MCP on the shape of the output signal. In Section 5 we present the test beam setup and the measurements that we performed. Discussion of the obtained results is presented in Section 6. The conclusions are given in Section 7.

2. Photonis XP85012 general properties.

We used the Photonis XP85012 (Fig. 1) with a separate HV wiring for PC, MCP and ground.

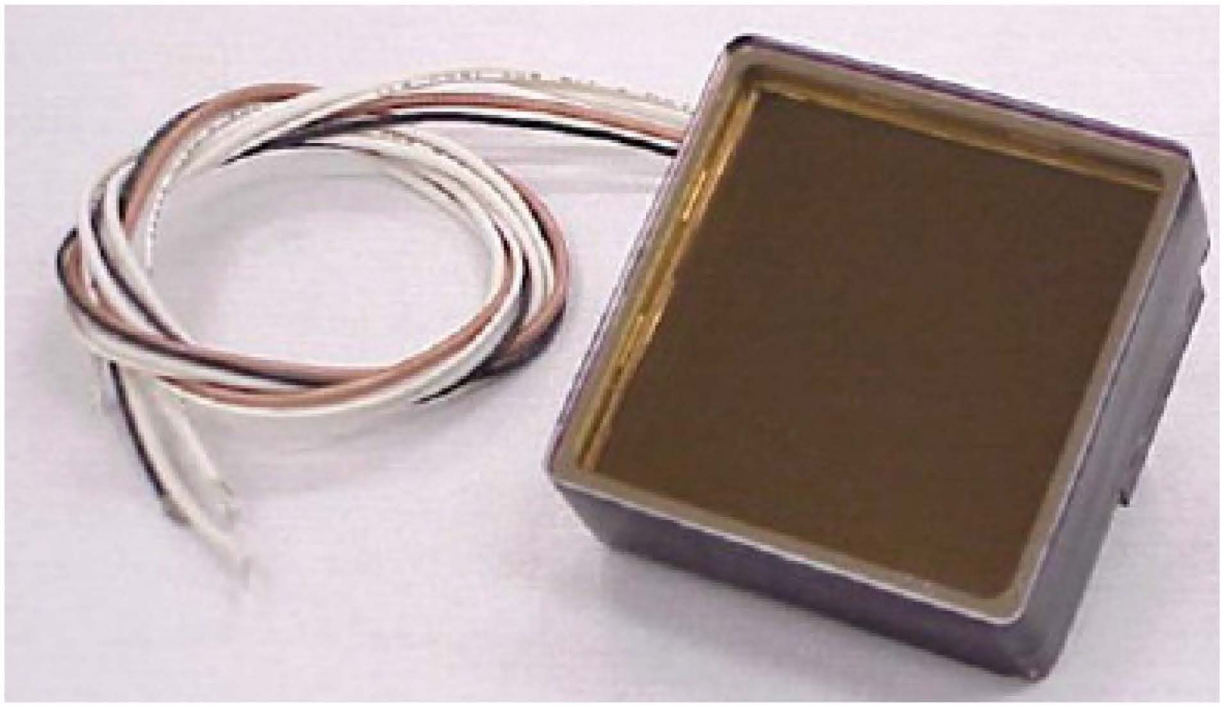

Fig. 1. External view of the Photonis XP85012.

The anode of the Photonis XP85012 is composed of 64 pixels, arranged as an 8x8 matrix (Fig. 2). Figure 1 and 2 were taken from the Photonis datasheet [8].

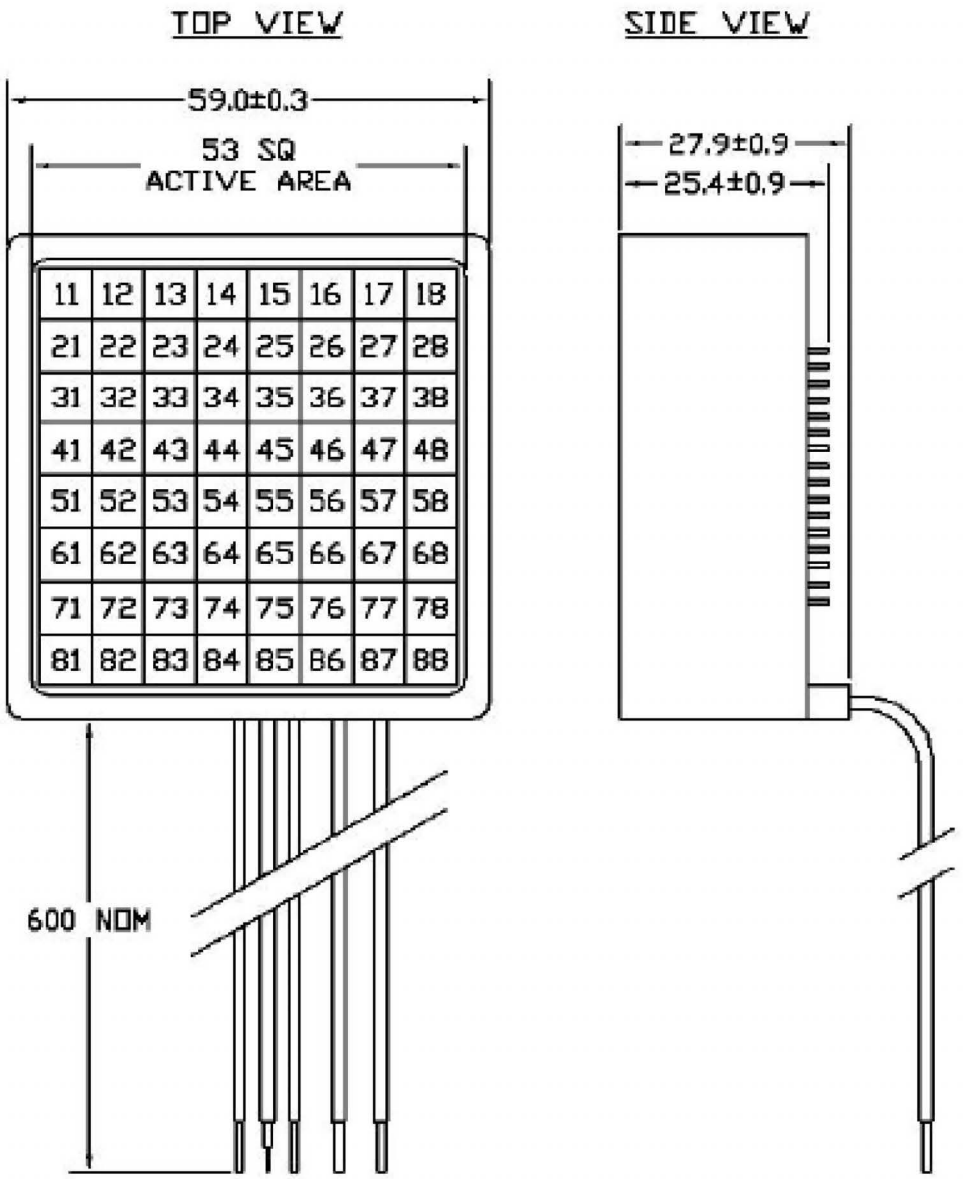

Fig. 2. Photonis XP85012 pixels schematics, top and side views.

The size of each pixel is ~6x6 mm^2. The sixteen central pixels (##33-36, ##43-46, ##53-56, ##63-66, forming a 4x4 matrix) were connected together to make a sensitive area of ~24x24 mm^2. The remaining 48 pixels were terminated by 50 Ohms. Timing non-uniformity along the photocathode, defined as the difference between the maximum and minimum of the signal delay among the sixteen channels with respect to the common trigger reference, was measured to be about 37 ps when using the passive sum of the 16 central pixels. The value was measured by illuminating a ~1 mm diameter spot across the photocathode and measuring the time interval between the PiLas laser [9] trigger and the Photonis XP85012 output signals. For this measurement we used electronics based on Ortec units [10].

3. Customized HV dividers for the Photonis XP85012 study.

A modified HV divider, shown in Fig. 3, was used to study the signal shape, and the dependence of the signal delay on the voltage applied between PC and MCP. The LEADER 718-5D floating power supply was used to adjust the potential between the PC and the MCP. The potential was scanned in the range of +17 and -17 Volts. The HV applied to the tube was 2.4 kV, with a corresponding gain of ~ 10^6. The PiLas laser with 405 nm (blue light) and 635 nm (red light) heads was used to illuminate the PC of the Photonis XP85012. The purpose of the modified HV schematics was to study the impact of the potential applied between the PC and the MCP on the signal shape.

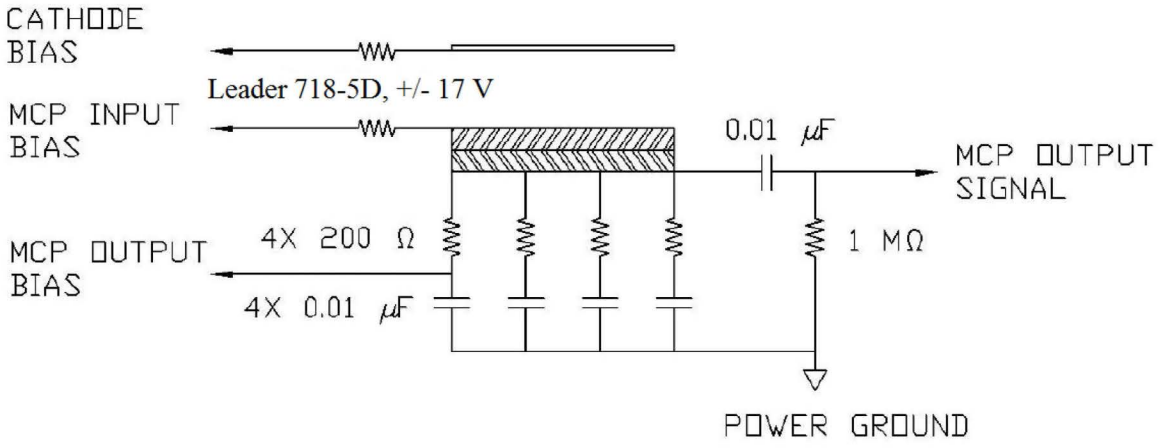

Fig. 3. Modified HV schematics.

We also produced a customized HV divider (Fig. 4). A 9V battery was used in the HV divider with a positive potential applied to the Photonis XP85012 PC to prevent any photoelectrons produced in the PC from reaching the MCP. This was possible by introducing a switch in the divider schematics (Fig. 4). The closed switch position corresponds to the PC ON operation, with negative potential applied to the photocathode relative to the MCP input. The PC OFF switch position corresponds to a +9 V potential applied to the PC relative to the MCP potential. This HV divider was used in our test beam measurements.

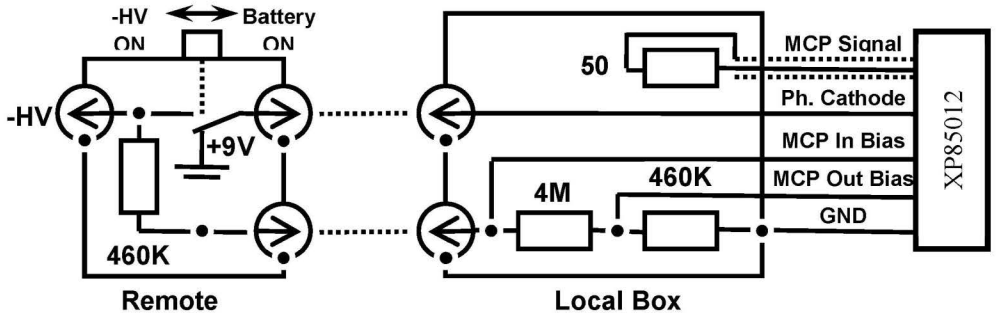

Fig. 4. Schematic Diagram of the customized HV divider.

4. Photonis XP85012 signal shape dependence on the applied potential.

To confirm that the 9V battery gives a potential difference that is sufficient to eliminate photoelectrons produced in the photocathode, we studied the dependence of the signal behavior in the Photonis XP85012 on the polarity and the applied potential using a PiLas laser. We made these measurements in accordance with the HV schematics presented in Fig. 3. The dependence of the signal shape on the potential value and polarity applied between the PC and the MCP is presented in Fig. 5. The traces were taken with a Tektronix TDS 3054B oscilloscope. The oscilloscope was triggered by the PiLas laser trigger signal. The horizontal and vertical scales are the same for all pictures below (4 ns/div, 100 mV/div), except for one (bottom right, 4 ns/div, 1 mV/div). The data were taken with both red and blue light illuminating the Photonis XP85012. One goal of the measurements was to observe possible differences in the Photonis XP85012 signal behavior depending on the potential difference for photons of different visible energies (~ 2 eV for red light and ~3 eV for the blue light). Fig. 5 illustrates the dependence of the signal shape on the magnitude and polarity of the potential applied between PC and MCP.

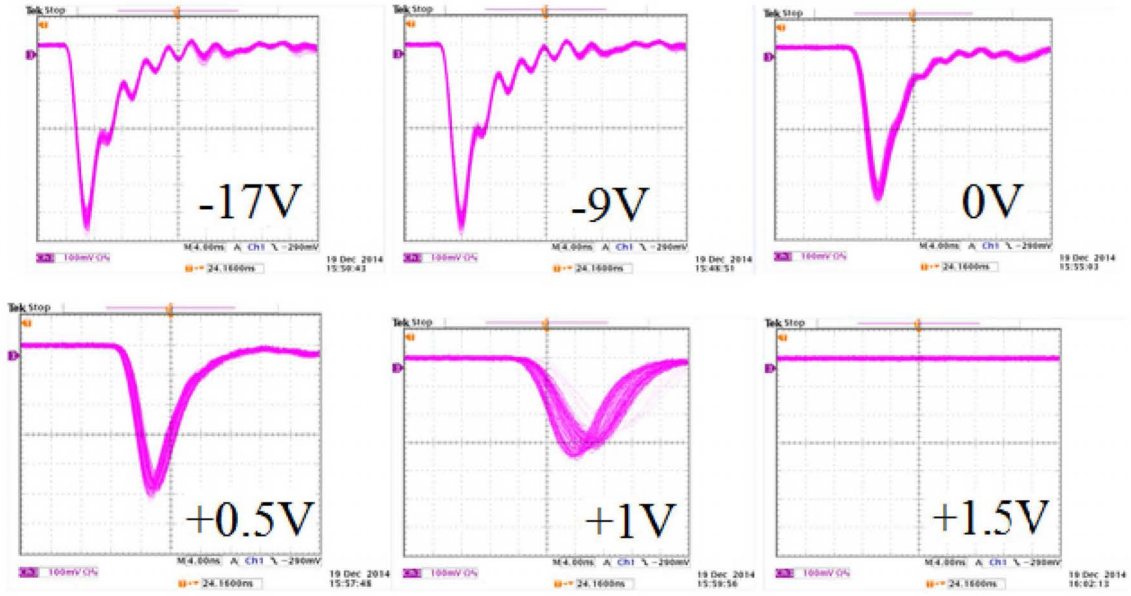

Fig. 5. Signal shape dependence on the value of the potential and the polarity between the PC and MCP. The Photonis XP85012, (PC is ON), was illuminated by red light (635 nm).

In Fig. 6 we present the dependence of the signal peak amplitude and its delay on the potential value and polarity between the PC and MCP. The measurements were done with both red (635 nm) and blue (405 nm) light. The data were extracted from the signal traces, some of which are presented in Fig. 5. We estimate the accuracy of the measurement as ~5% for the signal amplitude and ~ 0.3 ns for the signals time delay. The peak amplitude of the red light in Fig. 6 is lower because the amount of the light was not normalized and possibly due to lower quantum efficiency of the Photonis XP85012 for the red light. From Fig. 6, we observe that for both red and

blue light, the signal produced by photoelectrons from the PC is highly suppressed after applying a positive potential difference of 1.5V. Therefore, we conclude that the 9V battery used for the test beam setup is sufficient to eliminate the photoelectron signals from the PC.

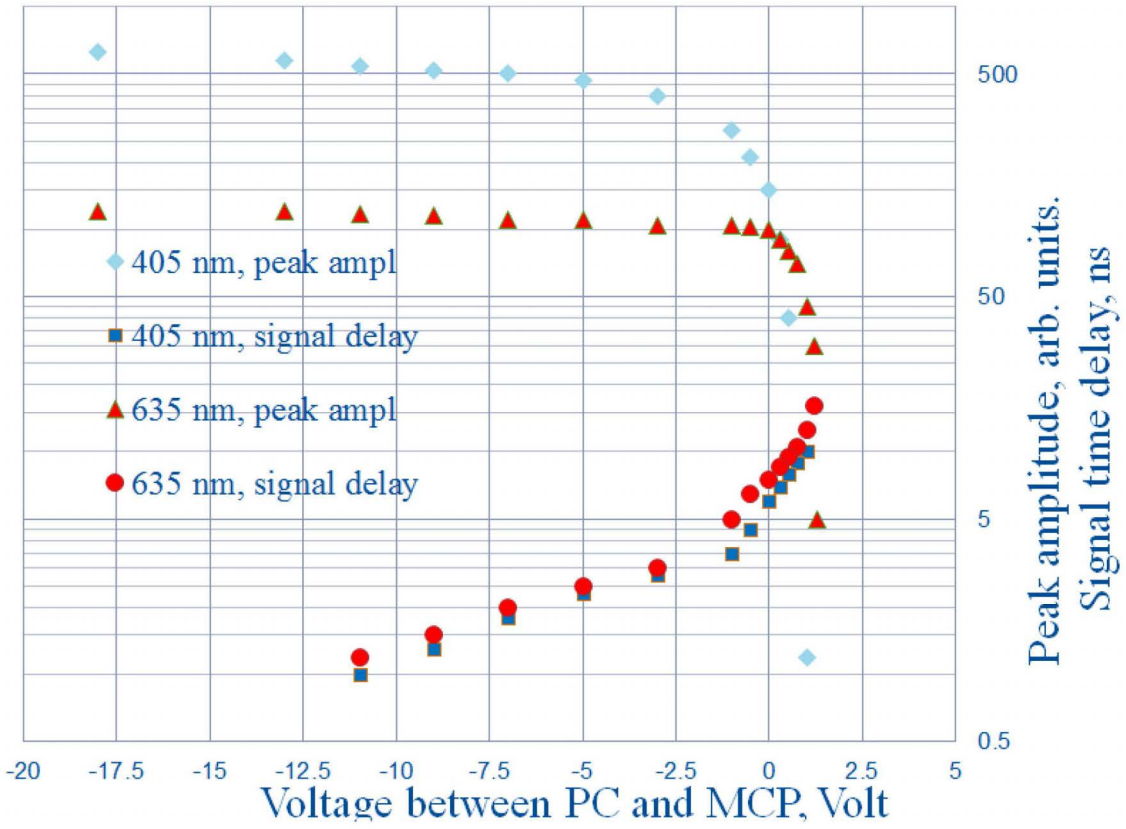

Fig. 6. The dependence of the peak amplitude and time delay of the signal on the value of the potential value and the polarity between the PC and MCP. The data were taken with blue (405 nm) and red (635 nm) laser lights.

5. Test beam setup and measurements.

The setup includes detectors placed inside a dark box, a data acquisition (DAQ) system based on DRS4 [11], HV power supplies, and equipment to monitor and control test beam parameters. The box was located on a moving table allowing us to change the dark box position both in the horizontal and vertical direction in the range of ~300 mm in X and Y with an accuracy better than 0.5 mm. Event selection and analysis was described in detail in [7]. The detectors were located inside of a dark box lined with copper foil for RF shielding (Fig. 7).

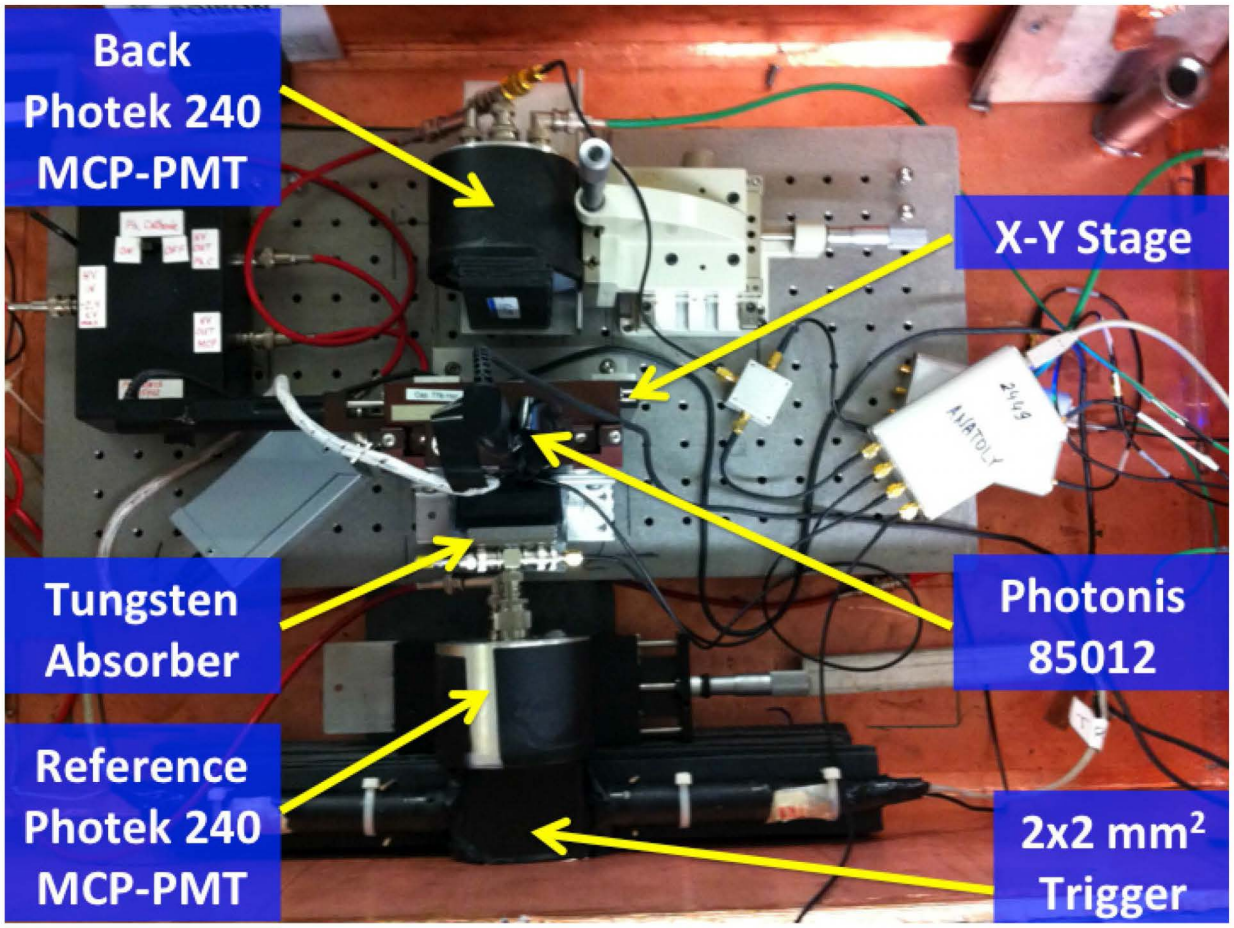

Fig. 7. Part of the test beam setup. Starting from the bottom: trigger counter, Photek 240, Photonis 85012, placed on X-Y moving stage and downstream Photek 240. A stack of tungsten plates can be seen upstream of the XP85012. A Cherenkov counter, located further upstream, is not shown in the picture.

Few changes to the setup were made with respect to previous work [7]. The trigger was based on a 1.7x2 mm^2 scintillation counter. The three detectors (two Photek 240 and the Photonis XP85012 between them) were placed in line. The Photonis XP85012 with tungsten absorber material of varying thicknesses was positioned on an X-Y moving stage, which allowed movement in both X and Y directions by ± 15 mm. The stage was operated remotely from the test beam control room. The accuracy of the Photonis XP85012 alignment was ~ 10 μm for both X and Y directions. The tungsten absorber material was used to initiate an electromagnetic shower when high energy electrons pass through.

Two DRS4 waveform digitizer units [11] performed the main readout. The DRS4 were triggered by TTL level signals originating from the trigger counter. Signals from the four detectors, two Photek 240, the Photonis XP85012 and the Cherenkov counter used for electron identification were split by high frequency Mini-Circuits ZFRSC-42-S+ splitters (4.2GHz BW). The outputs were connected in the same order to two DRS4 units. We attenuated the input signals (Photek 240

downstream and Photonis XP85012) to one of the two DRS4 units to cover the full dynamic range in the measurements. The other DRS4 did not have any additional attenuation. The schematic of the readout is described in detail in [7].

An example of a signal of the XP85012 recorded by DRS4 on the beam is shown in Fig. 8. Some ripples are seen after the signal, which is an effect due to connecting multiple anodes together. The signal rise time is ~ 2.3 ns.

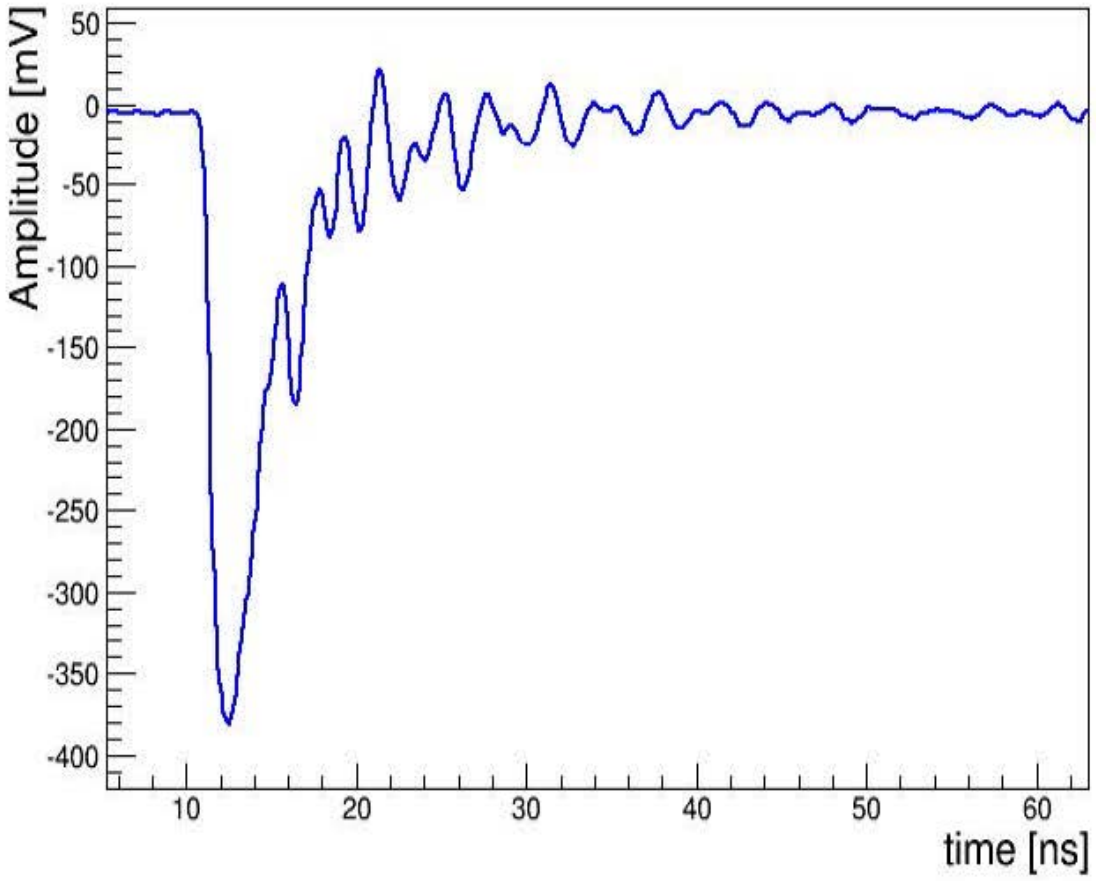

Fig. 8. Trace of the Photonis XP85012 recorded by DRS4 on the beam, 8 GeV electrons, 7 mm of tungsten upstream of the Photonis XP85012, the PC is OFF.

We can see large signal amplitude (377 mV) in the Fig. 8. The gain of the MCPs was in excess of 10^6. Placement of absorbers in front of the Photonis XP85012 also increased the signal size due to increased particle flux from secondary shower particles. We did not use any preamplifiers in the measurement.

We measured the "electronic" time resolution (TR) of the DRS4 taking into account the new calibration procedure [12]. The electronic time resolution was ~3.6 ps and has a negligible

impact on the measurements described in this article.

Most of the measurements were performed with an 8 GeV/c secondary beam because it provides a high purity electron beam, as well as to allow comparisons with our previous measurements with Photonis XP85011 MCP-PMT that were taken with an 8 GeV/c beam momentum. The stack of tungsten plates with different thicknesses was placed close to the Photonis XP85012 input window. The thickness of the input window is 2 mm. The transverse size of the tungsten plates allowed us to fully cover the transverse size of the MCP. For measurements with the secondary beams, we selected electron events with a gas Cherenkov counter that is part of the equipment provided by the Fermilab Test Beam Facility (FTBF). The fraction of the electrons in the 8 GeV secondary beam was ~50%.

In Fig. 9 we present the pulse height (PH) and time distribution of the Photonis XP85012 operated in the PC OFF mode, with 4 radiation lengths (X_0) of tungsten placed upstream of the XP85012. The radiation length Xo presented in mm. For the tungsten it is 3.5 mm.

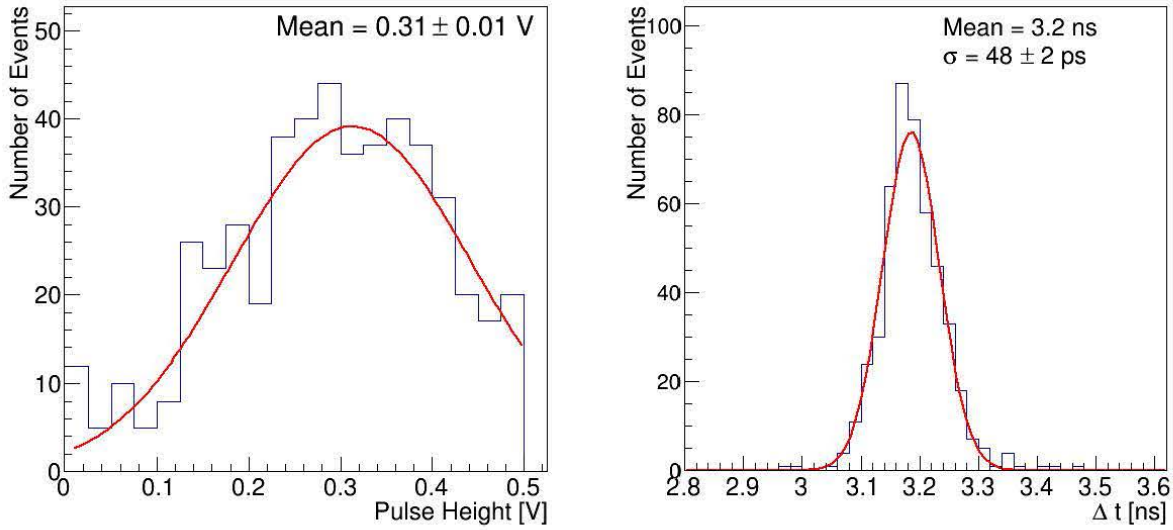

Fig. 9 Photonis XP85012 pulse height distribution (Fig. 9a, left), and the time difference between the XP85012 and the upstream Photek 240 (Fig. 9b, right). Conditions: 8 GeV, 4 Xo of tungsten before the Photonis XP85012, PC is OFF.

Fig. 10 presents the dependence of the MCP registration efficiency on the tungsten thickness in PC OFF mode. The efficiency is defined as the ratio:

$$\frac{N_{Photonis}}{N_{Photek}},$$

where $N_{Photonis}$ is the number of events with signal pulses from the Photonis XP85012 MCP with amplitude greater than 20 mV, and N_{Photek} is the number of events with signal pulses from the

upstream reference Photek 240 MCP with amplitude greater than 20 mV. We observe that the efficiency is very close to 100% for the range of the absorber thicknesses.

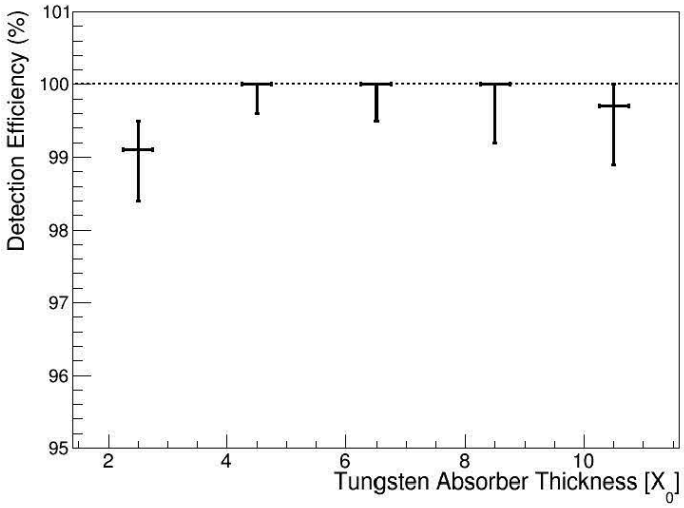

Fig. 10. Dependence of the MCP registration efficiency on the tungsten thickness in PC OFF mode.

Fig. 11 presents the time resolution of the Photonis XP85012 (PC ON and PC OFF) and its dependence on the thickness of the tungsten absorber. We do not observe significant variations of the measured time resolution as we vary the location in the shower depth sampled by the MCP.

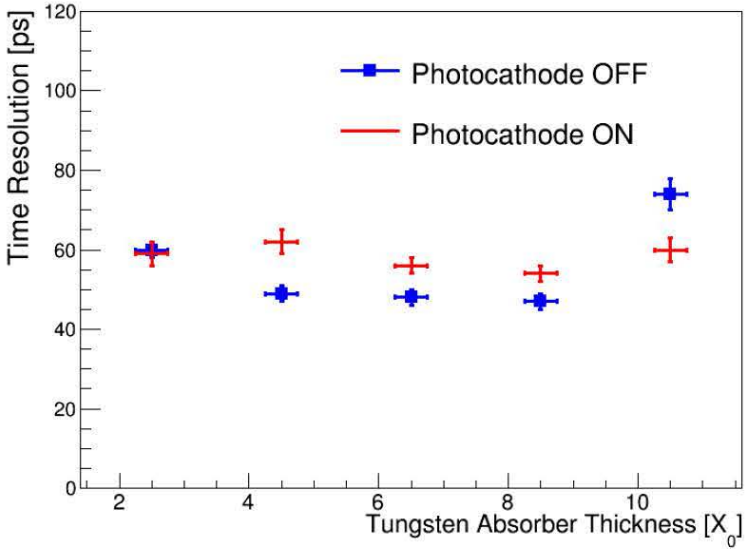

Fig. 11. Time resolution of the Photonis XP85012 (PC ON and PC OFF) and its dependence on the thickness of the tungsten absorber. Beams of 8 GeV electron were used.

In one short run with 32 GeV electrons we achieved a time resolution of 40 ± 1 ps. The time distribution is presented in Fig. 12. A better time resolution was obtained with 32 GeV electrons than with 8 GeV electrons (48 ± 2 ps, Fig. 9 b).

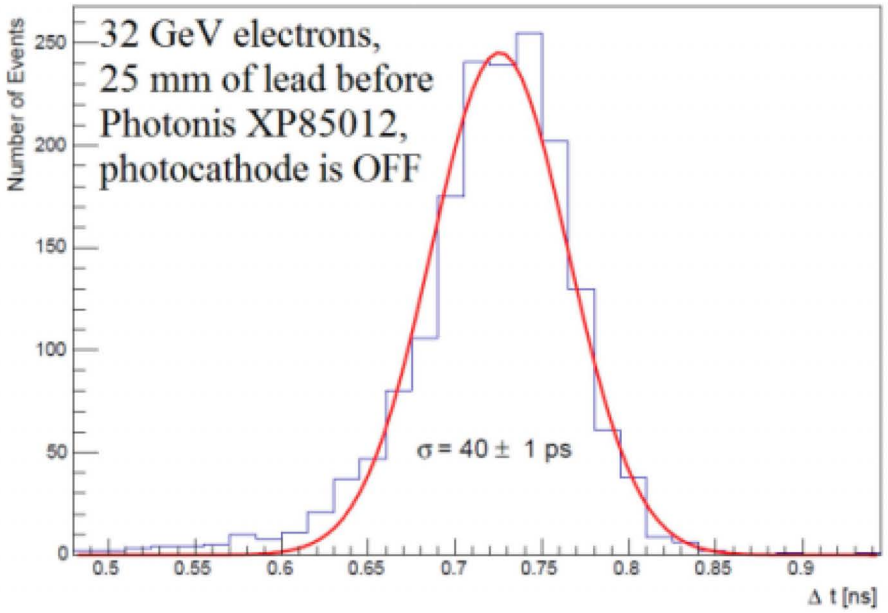

Fig. 12 Time resolution obtained under the following conditions: 32 GeV electrons, 25 mm of lead absorber placed before the Photonis XP85012 operated in the PC OFF mode.

6. Discussion.

The obtained data shows evidence that the secondary shower particles were registered through direct interaction with the MCP of the XP85012 while it was operated in the PC OFF mode. The time resolution of the secondary emission component can be estimated to be in the range of 47-60 ps for 8 GeV electrons. The MCP layer can be located in a wide range of the absorber thickness because of a rather flat time resolution dependence (Fig. 11). One run with 32 GeV electrons achieved a time resolution of 40 ps. These results indicate that the time resolution could be dependent on the beam energy and can improve with the energy increase for the same absorber thickness.

The degradation of the time resolution of the Photonis XP85012 with respect to the Photek 240 is primarily due to the passive sum of the 16 pixels, which exhibits 37 ± 1 ps time spread (difference between maximum and minimum signal delays with respect to PiLas laser signal) across the 24x24 mm^2 sensitive area. In comparison, the Photek 240 shows a time spread of only 4.7 ps across its 41 mm diameter sensitive area [10]. The better timing properties of the Photek 240 are due to the higher electric field between the PC and the MCP, and a smaller MCP pore diameter (10 μm compared to 25 μm for the Photonis 85012). The Photek 240 rise time was measured (with DRS4) to be more than a factor of two faster, at about 1 ns.

7. Conclusion.

We made direct measurements with the Photonis XP85012 MCP as a shower maximum detector. We used the XP85012 in two modes, one with its photocathode turned on primarily for calibration purposes, and one with its photocathode turned off. The measurements were performed at the Fermilab Test Beam Facility with 8 GeV/c and 32 GeV/c secondary beam momenta. With 8 GeV/c we obtained time resolution for the XP85012 operated in the PC OFF mode at the level of ~47 ps and close to a 100 % detection efficiency. The time resolution improves slightly with the electron energy increase. For the 32 GeV/c electrons the time resolution was measured to be 40 ps. This indicates a possibility for the further time resolution improvement with the energy increase.

We observe a slightly worse time resolution with the photocathode turned on. This could be a result of an additional jitter introduced by the photoelectron transit time. We do not observe a significant TR variation in a large range of the absorber thicknesses (from 2 X_0 to 11 X_0, Fig. 11). Therefore, the SM detector can be placed in a wide longitudinal range within an electromagnetic calorimeter.

The success of the LAPPD project [2] in developing affordable MCP's is encouraging in reducing the cost of such a SM detector. In our future experiments we plan to perform beam tests with MCPs (including the devices without photocathode) produced within the frame of the LAPPD project, utilizing different readout options. The SM detector based on the MCP approach can be economical, as well as very compact. It will occupy only a 1-2 cm gap within a calorimeter. Elimination of the photocathode from these devices will not only reduce the cost, but also significantly simplify their production. That will make the device much cheaper and more robust. This is also very important for the longevity of the detector, as one of the major reasons for MCP-PMT aging is the photocathode degradation [13].

Acknowledgment

We would like to thank Henry Frisch for useful discussions, Aria Soha and Eugene Smith for the good beam delivery and control, Ewa Skup for good working Cherenkov counter and Leo Bellantoni for using gap in his beam time. This work is supported by funding from Fermi Research Alliance, LLC under Contract No. DE-AC02-07CH11359 with the United States Department of Energy and from California Institute of Technology High Energy Physics under Contract DE-SC0011925 with the United States Department of Energy.

References

1. A. A. Derevschikov, V. Yu. Khodyrev, V. I. Kryshkin, V. E. Rakhmatov, A. I. Ronzhin., "On possibility to make a new type of calorimeter: radiation resistive and fast". Preprint IFVE 90-99, Protvino, Russia, 1990.

2. B. Adams, A. Elagin, H. Frisch, R. Obaid, E. Oberla, A. Vostrikov, R. Wagner, M. Wetstein., Nuclear Instruments and Methods A732 (2013) 392

3. A. I. Ronzhin, report, "Study of EM shower maximum detector for the STAR at RHIC, in: Proceedings of the "Notre Dame 1993, Scintillating Fiber Detectors", 1993, pp. 340–344.

4. S .A. Akimenko, V. I. Belousov, B. V. Chujko, A. A. Derevschikov, S. V. Erin, V.A. Kachanov, A. S. Konstantinov, I. V. Kotov, V. I. Kryshkin, N. G. Minaev, A. A. Morozov, A. I. Mysnik, V. L. Solovianov, V. I. Shelihov, K. E. Shestermanov, O. D. Tsai, A. N. Vasiliev, A. I. Ronzhin, V. L. Solovianov, V. I. Shelihov, K.E. Shestermanov, O. D. Tsay, A. N. Vasiliev., "Study of strip fiber prototype shower maximum detector for the STAR experiment at RHIC" Nuclear Instruments and Methods A365 (1995) 92-97

5. R. Wigmans, Calorimetry, Energy Measurement in Particle Physics, *International Series on Monographs on Physics*, Vol **107** (Oxford University Press) 2000.

6. R. Wigmans, and M. Zeyrek, Nuclear Instruments and Methods A485 (2002) 385

7. A. Ronzhin, S. Los, E. Ramberg, M. Spiropulu, A. Apresyan, S. Xie, H. Kim A. Zatserklyaniy ., "Development of a new fast shower maximum detector based on micro channel plates photomultipliers (MCP-PMT) as an active element" Nuclear Instruments and Methods in Physics Research A759 (2014) 65–73.

8. Photonis XP85012 Data Sheet: http://www.optimacorp.co.jp/Burle/Images/XP85012.pdf
9. PiLas Laser, Advanced Photonic Systems, A.L.S GmbH Schwarzschildstr 6, Photonic Center, D-12489 Berlin, Germany

10. A. Ronzhin, M.G. Albrow, M. Demarteau, S. Los, S. Malik, A. Pronko, E. Ramberg, A. Zatserklyaniy., "Development of a 10 ps level time of flight system in the Fermilab Test Beam Facility", Nuclear Instruments and Methods A623 (2010) 931-941.

11. S. Ritt, R. Dinapoli, U. Hartmann, Nuclear Instruments and Methods, A623 (2010) 486.

12. H. Kim, C.-T. Chen, N. Eclov, A. Ronzhin, P. Murat, E. Ramberg, S. Los, W. Moses, W.-S. Choong, C.-M. Kao., “A new time calibration method for switched capacitor-array-based waveform samplers”, Nuclear Instruments and Methods , A767 (2014) 67

13. M.Yu. Barnyakov and A.V. Mironov., “Photocathode aging in MCP PMT”, 2011 JINST 6 C12026, Workshop on fast Cherenkov detectors – Photon detection, DIRC design and DAQ April 4–6, 2011, Giessen, Germany